Anion Permeation in an Apical Membrane Chloride Channel of a Secretory Epithelial Cell

DAN R. HALM and RAYMOND A. FRIZZELL

From the Department of Physiology and Biophysics, University of Alabama at Birmingham, Birmingham, Alabama 35294

ABSTRACT Single channel currents though apical membrane Cl channels of the secretory epithelial cell line T84 were measured to determine the anionic selectivity and concentration dependence of permeation. The current–voltage relation was rectified with single channel conductance increasing at positive potentials. At 0 mV the single channel conductance was 41 ± 2 pS. Permeability, determined from reversal potentials, was optimal for anions with diameters between 0.4 and 0.5 nm. Anions of larger diameter had low permeability, consistent with a minimum pore diameter of 0.55 nm. Permeability for anions of similar size was largest for those ions with a more symmetrical charge distribution. Both HCO_3 and H_2PO_4 had lower permeability than the similar-sized symmetrical anions, NO_3 and ClO_4. The permeability sequence was $SCN > I \approx NO_3 \approx ClO_4 > Br > Cl > PF_6 > HCO_3 \approx F \gg H_2PO_4$. Highly permeant anions had lower relative single channel conductance, consistent with longer times of residence in the channel for these ions. The conductance sequence for anion efflux was $NO_3 > SCN \approx ClO_4 > Cl \approx I \approx Br > PF_6 > F \approx HCO_3 \gg H_2PO_4$. At high internal concentrations, anions with low permeability and conductance reduced Cl influx consistent with block of the pore. The dependence of current on Cl concentration indicated that Cl can also occupy the channel long enough to limit current flow. Interaction of Cl and SCN within the conduction pathway is supported by the presence of a minimum in the conductance vs. mole fraction relation. These results indicate that this 40-pS Cl channel behaves as a multi-ion pathway in which other permeant anions could alter Cl flow across the apical membrane.

INTRODUCTION

Secretion of chloride across many epithelial tissues is initiated by opening Cl channels in the apical membrane (Frizzell and Halm, 1990; Halm and Frizzell, 1990). Agents that produce an increase in intracellular cAMP are capable of activating secretion, in part through phosphorylation of Cl channels by protein kinase A. A 35–45-pS apical membrane Cl channel can be activated by protein kinase A in excised inside-out patches (Schoumacher, Shoemaker, Halm, Tallant, Wallace, and Frizzell, 1987; Li,

Address reprint requests to Dr. Dan R. Halm, Department of Physiology, Ohio State University, 1645 Neil Avenue, Columbus, OH 43210-1218.

J. GEN. PHYSIOL. © The Rockefeller University Press · 0022-1295/92/03/0339/28 $2.00
Volume 99 March 1992 339–366

McCann, Liedtke, Nairn, Greengard, and Welsh, 1988). Single channel conductance and open probability for this channel increase as the membrane electrical potential difference is made more positive (Halm, Rechkemmer, Schoumacher, and Frizzell, 1988*a*). Cl channels with these characteristics have been observed in cells from several secretory epithelia (Frizzell and Halm, 1990), indicating that this Cl channel may play a role in Cl secretion, together with other types of Cl channels that also appear to be involved. A 9-pS voltage-insensitive Cl channel can be activated by cAMP-dependent secretagogues in T84 cells (Tabcharani, Low, Elie, and Hanrahan, 1990), and a 20-pS Cl channel was observed in airway epithelial cells (Duszyk, French, and Man, 1990). Whole-cell currents measured in T84 cells also indicate the presence of two distinct types of Cl conductance (Cliff and Frizzell, 1990). The relative contribution of each of these Cl channels to transepithelial Cl secretion under various stimulatory conditions remains to be determined.

Flow of Cl through any channel depends on the properties of the channel, including single channel conductance, open probability, and other modulating factors. Secretion of HCO_3 also may be electrogenic in some epithelia (Stewart, Winterhager, Heintze, and Peterson, 1989), consistent with the presence of apical membrane HCO_3 conductance. The results reported here indicate that physiologically relevant anions, such as HCO_3, are less permeant than Cl but can alter Cl flow through this 40-pS channel. The dependence of single channel conductance on Cl concentration and permeant anions is indicative of anion interaction within the conduction pathway. Interactions of this type may allow for modulation of Cl exit by alterations in cell pH or energy metabolism.

METHODS

T84 cells were obtained from K. Dharmsathephorn and J. McRoberts (University of California San Diego) at passage 12 and studied from passage 14 to 65. Cells were grown in a 1:1 mixture of Dulbecco's minimal essential medium and Ham's F12 plus 5% bovine calf serum (Halm et al., 1988*a*). Cells grown on coverslips were transferred to a chamber mounted on the stage of an inverted microscope. Simple electrolyte solutions bathed the cells in the chamber. The standard bathing solution was (mM): 155 Na, 161 Cl, 5 Mg, 0.5 Ca, 1 EGTA, and 5 HEPES. The calculated Ca activity was 200 nM. The standard pipette filling solution was (mM): 162 Na, 164 Cl, 2 Ca, and 5 HEPES. All solutions were titrated to pH 7.2. Solutions with Cl replaced by other anions maintained the sum of Cl and substitute anion (A) at 161 mM, generally 150 mM A and 11 mM Cl. Changes in Cl concentration were made by raising or lowering the NaCl concentration of the standard solution. During most studies the cells were at ambient temperature, 20–22°C. Temperature dependence of channel currents was examined by using a Peltier device to warm or cool the bath chamber. Currents and temperature were monitored while the bathing solution returned to ambient. The relaxation rate was ~0.5°C/min.

Currents were recorded using an EPC-5 amplifier (Medical Systems Corp., Greenvale, NY) in both cell-attached and inside-out recording configurations. Pipettes were fabricated from Corning glass 8161 (Corning Glass Incorporated, Corning, NY) using a two-stage pipette puller (Narishige USA, Inc., Greenvale, NY) followed by a coating with Q-dope. The pipette resistances were 1–2 MΩ when filled and immersed in the bath. Connections to the amplifier were made via Ag/AgCl pellets and KCl-agar bridges. All electrical potential differences are expressed with the pipette solution as reference; positive currents are those flowing from the

inside (cytoplasmic side) of the membrane to the outside. Current output from the amplifier was filtered at 1 kHz. Both current and voltage outputs were recorded on video tape after A/D conversion by a modified pulse code modulation device (A. R. Vetter Co., Rebersburg, PA). Cl channels were activated irreversibly in excised inside-out patches by holding the patch potential at +40 to +80 mV for 30 s to several minutes (Halm et al., 1988*a*).

Single channel currents were measured on the screen of an INDEC lab computer (Sunnyvale, CA). Current–voltage relations were plotted to determine reversal potentials for current flow. Junction potentials evoked by changes in bath composition were calculated using the Henderson approximation of the Nernst-Planck equation. Relative ion permeabilities were calculated from the reversal potentials using the Goldman-Hodgkin-Katz (GHK) equation, after correction for junction potentials.

RESULTS

Temperature Dependence

Single channel currents were recorded at bath temperatures ranging from 9 to 38°C. Cl channel activity was obtained first in inside-out excised patches at ambient

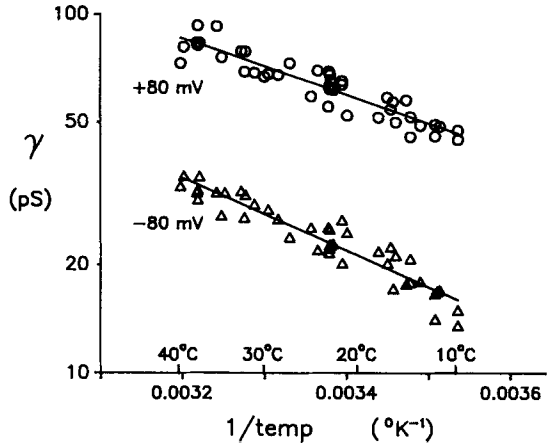

FIGURE 1. Temperature dependence of single channel conductance. Arrhenius plots are shown for single channel chord conductance at +80 mV (○) and −80 mV (△). The points are from nine experiments, four in which the patches were cooled to 9°C and five in which the patches were warmed to 38°C. The slopes of the linear fits gave apparent activation energies that correspond to Q_{10} values of 1.2 at +80 mV and 1.3 at −80 mV.

temperature. Activity was monitored further after the bath was warmed to 38°C or cooled to 9°C. Acquisition of current–voltage relations required ~60 s, allowing measurement of single channel conductance at several temperatures during the relaxation to ambient temperature. The kinetics of channel opening and closing were not easily discerned because two or three channels generally were present in the records; however, open probability was not noticeably dependent on temperature. Single channel conductances at +80 and −80 mV are shown in Fig. 1 as an Arrhenius plot, with apparent activation energies of 3.6 and 4.7 kcal/mol, respectively. These values are consistent with activation energies for ion diffusion in aqueous solutions (Robinson and Stokes, 1970) and in ion channels (Bamberg and Läuger, 1974; Hille, 1991).

Dependence on Internal pH

Current–voltage relations were obtained from Cl channels in excised inside-out patches at bath pH's of 6.0, 7.2, 8.0, and 9.0. The buffer used was BIS-TRIS propane (5 mM) rather than HEPES because of the wider buffering range of this divalent cationic buffer. The current–voltage relation at pH 7.2 was identical to that with HEPES, as noted previously (Halm et al., 1988*a*). Fig. 2 shows the single channel currents for positive and negative potentials over a range of internal pH (external pH constant at 7.2). Conductance at positive and negative potentials increased at acidic pH and decreased at basic pH. The slope for this relation was 9 pS/pH unit at −80 mV (between pH 6 and 8) and 7 pS/pH unit at +80 mV. The apparent pK_a of this relation is 7.1 or less, and a significant portion (~60%) of the single channel conductance appears pH insensitive.

Anion Selectivity

Halide permeabilities determined from reversal potentials have a sequence I > Br > Cl > F (Halm et al., 1988*a*), suggesting that interactions of larger anions with the channel are more optimal than for smaller anions. Relative permeabilities of other anions were measured similarly in excised inside-out patches from reversal potential shifts of single channel current–voltage relations after anion substitutions in the bath (cytoplasmic or internal side) solution. Ions tested included polyatomic anions with different geometries of charge distribution and with nonpolar side chains of different sizes (Table I). Fig. 3 shows the relative permeabilities for polyatomic anions together with the halide values. Ionic size for the polyatomic anions was estimated from CPK models and plotted as the geometric mean diameter (Dwyer, Adams, and Hille, 1980). This representation illustrates that ions of similar size are not equally permeant, suggesting that the charge distribution of the ion influences interaction within the channel.

Reversal potentials with Cl in the bath and the test anion in the pipette were obtained for Br, F, SCN, NO_3, and ClO_4. These measurements gave relative permeabilities identical to those obtained with substitution of the test ion in the bath (Table I). This result indicates that these relative permeabilities are voltage insensitive over the relatively narrow range spanned by the reversal potentials for these anions (from about −20 to +20 mV).

Together with bicarbonate and phosphate, short-chain fatty acids (SCFAs) are biologically relevant anions, particularly in the large intestine where luminal concentrations of acetate can be 50 mM (Wrong, Edmonds, and Chadwick, 1981). SCFAs vary primarily in the length of the hydrocarbon side chain, and lactate, pyruvate, and 2-methyl propanoate differ from propanoate in substitutions for a hydrogen on the second carbon with hydroxyl, oxo, and methyl groups, respectively. Gluconate differs from hexanoate by having hydroxyls substituted along the length. A series of sulfonates were also tested: methane sulfonate, ethane sulfonate, 1-propane sulfonate, and 2-propane sulfonate. Because many of these organic ions are roughly linear, dimensions also were estimated from the smallest cylinder that enclosed the molecule. The dependence of SCFA permeation on size followed the cylindrical diameter more closely than either the length or a spherical approximation; therefore,

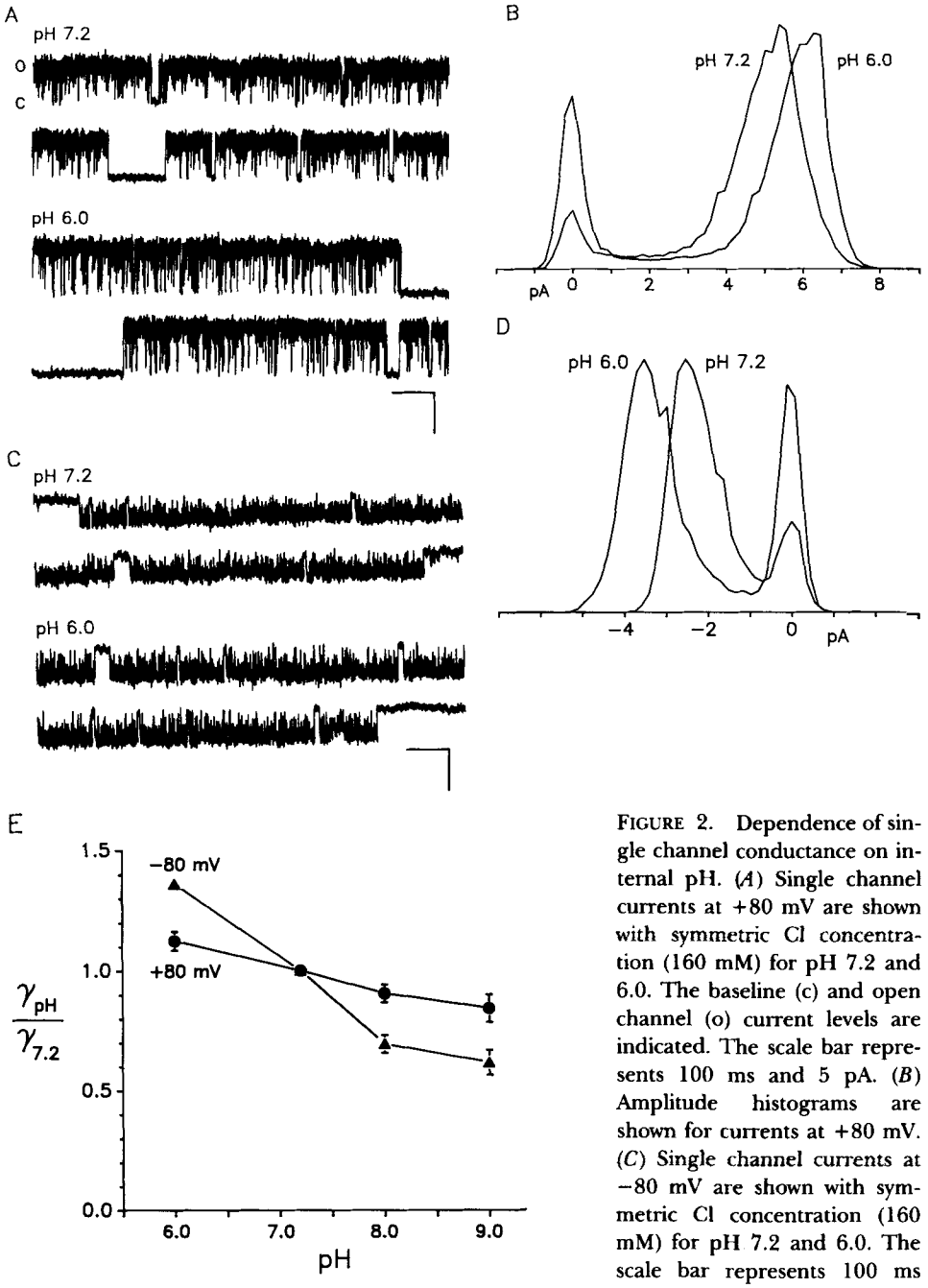

FIGURE 2. Dependence of single channel conductance on internal pH. (*A*) Single channel currents at +80 mV are shown with symmetric Cl concentration (160 mM) for pH 7.2 and 6.0. The baseline (c) and open channel (o) current levels are indicated. The scale bar represents 100 ms and 5 pA. (*B*) Amplitude histograms are shown for currents at +80 mV. (*C*) Single channel currents at −80 mV are shown with symmetric Cl concentration (160 mM) for pH 7.2 and 6.0. The scale bar represents 100 ms and 5 pA. (*D*) Amplitude histograms are shown for currents at −80 mV. (*E*) The chord conductance was measured from current–voltage relations (n = 6) at +80 mV (●) and −80 mV (▲) and plotted relative to the value at pH 7.2. The chord conductance at pH 7.2 was 26 ± 1 pS and 72 ± 2 pS at −80 mV and +80 mV, respectively.

the data were plotted in Fig. 3 according to cylindrical diameter. Trimethylacetate (TMA) and trichloroacetate (TCA) are roughly spherical with diameters of 0.60 and 0.62 nm, respectively. The relative permeability of TMA was near zero, and though a reversal potential was not observed with TCA substitution, outward currents at negative potentials were similar to those with TMA substitution, suggesting insignificant permeability for TCA.

TABLE I

Ion Selectivity

	P_X/P_{Cl}	n	γ_X/γ_{Cl} Anion efflux (negative potential)	γ_X/γ_{Cl} Anion influx (positive potential	n
SCN	2.06 ± 0.04	9	1.29 ± 0.05‡	0.92 ± 0.03‡§	5
I	1.74 ± 0.04	11	0.99 ± 0.05*‡	0.78 ± 0.05‡§	3
NO_3	1.73 ± 0.04	9	1.56 ± 0.05‡	1.10 ± 0.04‡§	4
ClO_4	1.70 ± 0.02	6	1.20 ± 0.03‡	0.91 ± 0.03‡§	3
Br	1.39 ± 0.03	14	0.99 ± 0.07*‡	0.88 ± 0.05*‡	3
Cl		1.00	1.00	1.00	
PF_6	0.95 ± 0.02*	3	0.78 ± 0.02‡	—	3
Formate	0.76 ± 0.03	3	0.53 ± 0.06‡	—	3
Methane SO_3	0.53 ± 0.01	3	0.41 ± 0.01‡	—	3
Acetate	0.49 ± 0.01	3	0.39 ± 0.05	—	3
Pyruvate	0.49 ± 0.04	3	0.34 ± 0.02‡	—	3
Ethane SO_3	0.47 ± 0.09	3	0.31 ± 0.03	—	3
HCO_3	0.44 ± 0.02	5	0.38 ± 0.04	—	3
1-Propane SO_3	0.43 ± 0.03	3	0.29 ± 0.02‡	—	3
Propanoate	0.42 ± 0.03	6	0.33 ± 0.05	—	5
2-Propane SO_3	0.41 ± 0.02	3	0.30 ± 0.02‡	—	3
F	0.39 ± 0.02	5	0.41 ± 0.02	0.56 ± 0.06‡	3
Hexanoate	0.38 ± 0.06	3	0.15 ± 0.02‡	—	3
Butanoate	0.37 ± 0.02	3	0.23 ± 0.01‡	—	3
2-Methyl propoanoate	0.31 ± 0.03	3	0.23 ± 0.02	—	3
L-Lactate	0.30 ± 0.04	3	0.21 ± 0.01‡	—	3
Gluconate	0.14 ± 0.05	4	0.13 ± 0.02	—	3
H_2PO_4	0.06 ± 0.06	3	0.02 ± 0.02	—	3
Trimethylacetate	0.03	1	—	—	—
Na	0.02 ± 0.01	[1]	—	—	—

Mean ± SEM. P_X/P_{Cl} was calculated with the GHK equation from reversal potential shifts determined with single-sided substitution of the test ion in the bath. γ_X/γ_{Cl} at −80 and +80 mV was determined from single channel conductance with symmetric substitution (SCN, I, NO_3, ClO_4, Br, F) or at −68 mV (E_{Cl}) from conductance of inward current with single-sided substitution (all others). Those values not significantly different ($P < 0.05$) from the Cl value are indicated (*). γ_X/γ_{Cl} significantly different ($P \leq 0.05$) from P_X/P_{Cl} are indicated (‡). $\gamma_X\gamma_{Cl}$ for anion influx significantly different ($P \leq 0.05$) from γ_X/γ_{Cl} for anion efflux are indicated (§). [1]Halm et al., 1988*a*.

Ion selectivity was also determined from single channel currents measured with the test anion substituted symmetrically for Cl (Fig. 4 *A*). Substitution with these more permeant anions often led to the appearance of several identically sized current levels, suggesting that these kaotropic anions can activate this channel. Fig. 4 *B* shows

the relative single channel conductance for symmetrical halide and polyatomic anion substitutions (see Table I for values at ±80 mV). These relative conductances were voltage dependent with discrimination among the anions decreasing from a maximum extent of fourfold at −100 mV to twofold at +100 mV.

Conductances for the less permeant anions were estimated from the current–voltage relations obtained with single-sided substitution (those used to determine reversal potentials). In these experiments the equivalent electromotive force for Cl was −68 mV, so that currents measured at that potential are due to the substitute anion. These currents were compared with similarly obtained values for Br to obtain a relative conductance (γ_X/γ_{Br}) and multiplied by the Br conductance relative to Cl ($[\gamma_X/\gamma_{Br}][\gamma_{Br}/\gamma_{Cl}]$) to make the conductance comparison directly with Cl (Table I). Though the larger SCFAs had similar relative permeabilities, the relative conduc-

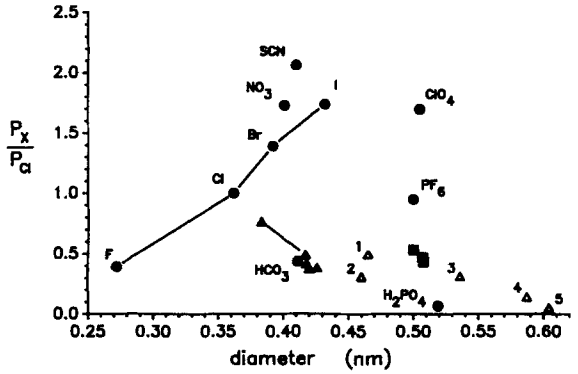

FIGURE 3. Relative permeabilities of polyatomic anions. Reversal potentials were obtained with single-sided substitution of the test ion, and relative permeabilities were calculated from the GHK equation (Table I). Ionic diameter was estimated from CPK models (Dwyer et al., 1980). The short chain fatty acids (▲) were approximated by a cylinder and plotted as the cylindrical diameter (with increasing size: formate, acetate, propanonate, butanoate, hexanoate). Also shown are the sulfonates (■) and derivatives of the SCFAs (△): 1, pyruvate; 2, lactate; 3, 2-methyl propanoate; 4, gluconate; 5, trimethylacetate. The pH of the H_2PO_4 and HCO_3 solutions were changed to pH 6.0 and 8.5, respectively, to have these anions primarily in the monovalent form. For the phosphate solution 94% of the phosphate was monovalent. With carbonate, 98% was monovalent so that loss of HCO_3 as CO_2 was minimal.

tances decreased with increasing size of the side chain. This relationship to the extended length of the anion can be seen in Fig. 4 *C*. Sulfonates with lengths similar to the SCFAs had nearly identical conductances, suggesting a steric restriction due to the orientation of a long side chain. Relative conductances generally were lower than relative permeabilities (Fig. 4 *D*). Large deviations from the line of identity are consistent with high affinity for a site in the channel that impedes rapid passage of that anion.

Dependence of Single Channel Conductance on Cl Concentration

The dependence of Cl flow on Cl concentration was obtained in inside-out patches bathed with symmetrical Cl concentrations. Patches were obtained with each Cl concentration as the pipette solution and with the standard bath solution. After

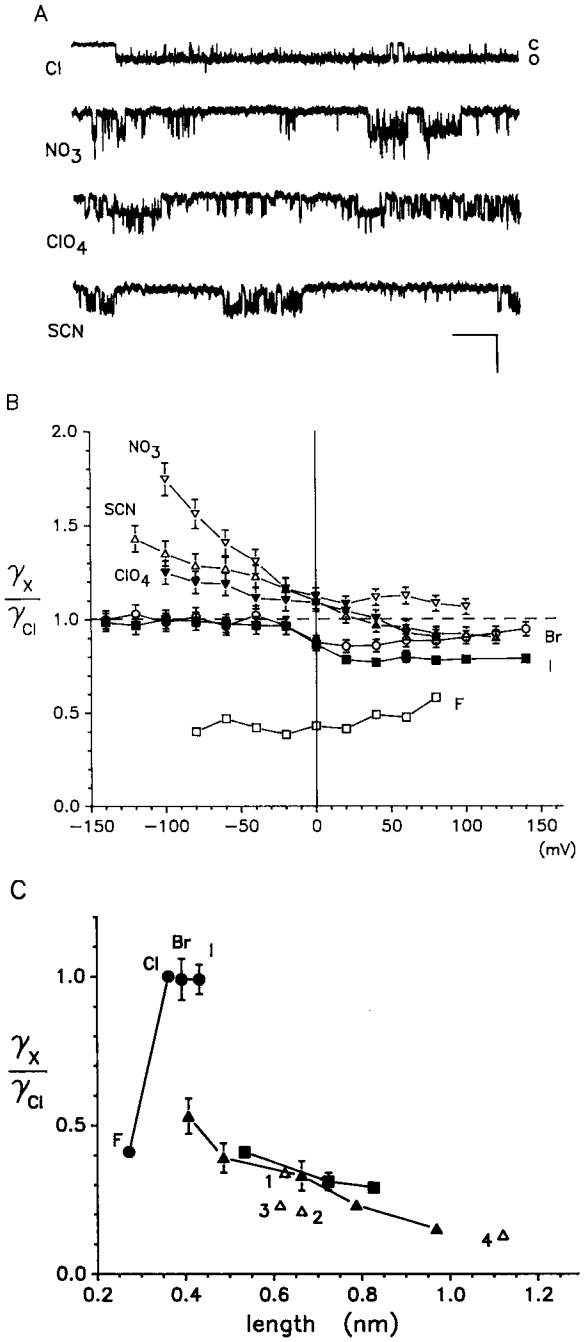
A
Cl
C
O
NO3
ClO4
SCN
B
2.0
1.5
1.0
0.5
0.0
NO3
SCN
ClO4
Br
I
F
−150
−100
−50
0
50
100
150
(mV)
C
1.0
0.5
0.0
Cl
Br
I
F
1
2
3
4
0.2
0.4
0.6
0.8
1.0
1.2
length (nm)

obtaining Cl channel activity, the bath was changed to the symmetric Cl concentration. Single channel chord conductances at four Cl concentrations are shown in Fig. 5 *A*, and conductance increased toward positive voltages at all Cl concentrations. The relations of conductance to Cl activity (Fig. 5 *B*) exhibit nonlinear behavior at negative potentials.

The shape of these conductance–activity relationships (Fig. 5 *B*) may depend on surface charges which could redistribute ions in the vicinity of the channel (Dani, 1986; Dani and Eisenman, 1987; Green, Weiss, and Andersen, 1987), because ionic strength was not held constant as NaCl concentration was changed. Maintaining ionic strength at 300 mM by adding Na gluconate did not alter the conductance with 160

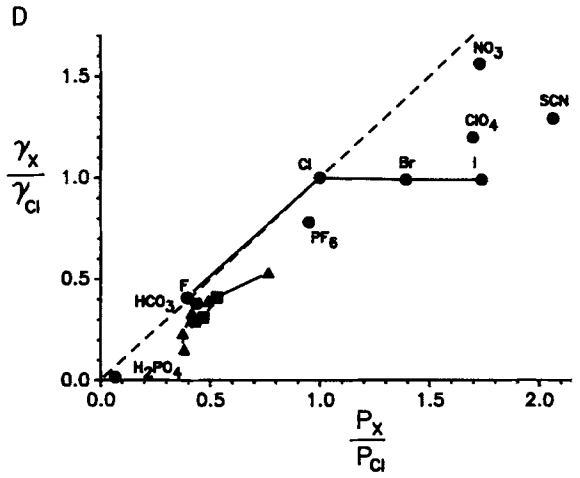

FIGURE 4. Single channel conductance of anions. (*A*) Single channel currents at −80 mV are shown with Cl substituted by other anions in both bath and pipette solutions. The scale bar represents 100 ms and 5 pA. (*B*) The conductance–voltage relation is shown. Conductances relative to Cl were calculated by comparing current–voltage relations with symmetric test ion to the case with symmetric Cl. The values at +80 and −80 mV are shown in Table I. (*C*) The relative conductances of organic anions are plotted versus extended length (▲, SCFAs; ■, sulfonates; 1, pyruvate; 2, lactate; 3, 2-methyl propanoate; 4, gluconate). The halides are plotted, for comparison, according to ionic diameter. (*D*) Comparison of relative conductances and permeabilities is shown. The relative conductances are those for anion efflux (Table I). Comparing the ratio of relative permeability to relative conductance ($[P_X/P_{Cl}]/[\gamma_X/\gamma_{Cl}]$) allows a rough estimate of the sequence for relative affinity (Läuger, 1973), which would be complicated by different selectivities at each barrier or multiple occupancy. The sequence of these apparent affinities (during efflux) is I ≈ SCN > ClO_4 ≈ Br > HCO_3 ≈ NO_3 > Cl > F. Hexanoate has the largest apparent relative affinity of the anions studied and the strongest block (Fig. 10).

mM Cl. Increased ionic strength did increase conductance with 60 mM Cl by 23% (2 pS) at −80 mV, but not at positive potentials. This increase of conductance with 60 mM Cl at high ionic strength may be due to screening of negative surface charge that thereby increased the local Cl concentration; however, the conductance of gluconate, present at 250 mM, may contribute to this small increase of conductance.

The nonlinear dependence of conductance on Cl concentration at negative potentials is consistent with a site within the conduction pathway that when occupied impedes flow of other anions. An Eadie-Hofstee plot of the conductances (Fig. 5 *C*) illustrates that the data are not consistent with either a single interaction site in the Henri-Michaelis-Menten formalism or independence of flow as occurs in simple

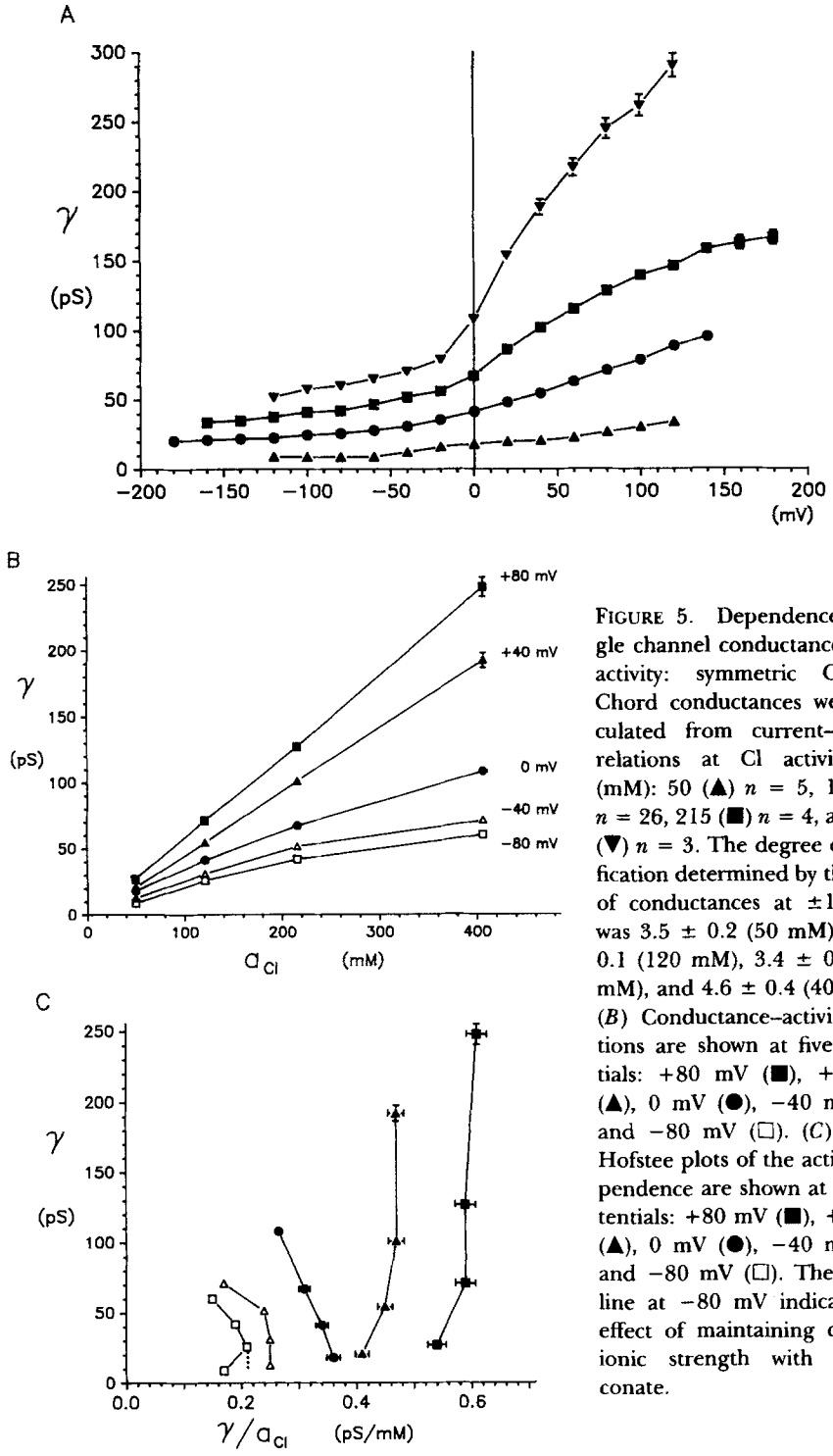

FIGURE 5. Dependence of single channel conductance on Cl activity: symmetric Cl. (*A*) Chord conductances were calculated from current–voltage relations at Cl activities of (mM): 50 (▲) n = 5, 120 (●) n = 26, 215 (■) n = 4, and 405 (▼) n = 3. The degree of rectification determined by the ratio of conductances at ±100 mV was 3.5 ± 0.2 (50 mM), 3.3 ± 0.1 (120 mM), 3.4 ± 0.2 (215 mM), and 4.6 ± 0.4 (405 mM). (*B*) Conductance–activity relations are shown at five potentials: +80 mV (■), +40 mV (▲), 0 mV (●), −40 mV (△), and −80 mV (□). (*C*) Eadie-Hofstee plots of the activity dependence are shown at five potentials: +80 mV (■), +40 mV (▲), 0 mV (●), −40 mV (△), and −80 mV (□). The dotted line at −80 mV indicates the effect of maintaining constant ionic strength with Na-gluconate.

diffusion through dilute solutions. The expectation for a simple one-site process would be a straight line that intercepts the ordinate at the maximal conductance and has a negative slope equal to the activity for half saturation. Curvature of the relations at negative voltages (Cl efflux) suggests multiple sites of interaction and the vertical lines at positive voltages (Cl influx) are consistent with simple diffusion. Extrapolation of the relation at negative voltages suggests an apparent maximal conductance of ~120 pS, which corresponds to an apparent activity for half saturation of ~400 mM.

Dependence of conductance on Cl concentration was also examined with asymmetric Cl concentrations. Cl was held constant at 160 mM on either the external or internal face of the membrane patch, while varying the Cl on the opposite side. The current–voltage relations for constant external Cl are shown in Fig. 6 *A*, with increased internal Cl producing increased Cl efflux (inward current). The current–voltage relations for constant internal Cl are shown in Fig. 7 *A*, with increased external Cl producing increased Cl influx (outward current). These increases in current with increases in *cis* Cl concentration, the concentration on the side from which Cl is flowing (Fig. 8), provide evidence for saturating behavior of conductance at both positive and negative voltages when examined with Eadie-Hofstee plots. Though far from actual saturation, these conductances clearly deviate from the expectations for independence of flow (relations with infinite slope, in Fig. 8 *B*). An Henri-Michaelis-Menten fit of the conductances at +80 mV gave an apparent maximal conductance of 250 pS and an activity for half saturation of 310 mM. Extrapolation of the relation at −80 mV suggests a maximal conductance of 200–250 pS with a corresponding activity for half saturation of ~1,000 mM. This difference in apparent affinity is consistent with a greater likelihood for prolonged channel occupancy by Cl during Cl influx than for Cl efflux. These results contrast with those obtained with symmetric Cl concentration increases (Fig. 5), which indicated that prolonged occupancy was more likely for Cl efflux than for Cl influx.

The current–voltage relations in Figs. 6 and 7 also show the dependence of current on *trans* variations in Cl concentration, the concentration on the side toward which Cl is flowing. With *cis* Cl concentration constant, *trans* changes altered Cl influx (outward current) but not Cl efflux (inward current), which suggests that internal Cl can modify Cl influx. These results were identical whether HEPES or BIS-TRIS propane was the buffer, indicating further that the anionic buffer HEPES does not have a major influence on Cl flow in this channel. Single channel currents and amplitude histograms illustrate this *trans* stimulation by internal Cl (Fig. 6, *B* and *C*). The ability of *trans* Cl to alter Cl flow is seen best by subtracting the currents observed with symmetric 160 mM NaCl from the currents in the gradient conditions. For a simple channel obeying independent flow of ions, these difference currents (Figs. 6 *D* and 7 *B*) would be expected to asymptotically approach zero as voltage is applied to drive Cl from the side with 160 mM NaCl (at positive voltages in Fig. 6 *D* and at negative voltages in Fig. 7 *B*). This notion qualitatively describes Cl efflux (inward current) with external Cl changes (Fig. 7 *B*): at positive voltages current was larger with 300 mM Cl and smaller with 60 mM Cl, while at negative voltages the currents became indistinguishable. However, Cl influx (outward current) clearly is larger when internal Cl is higher and smaller when internal Cl is lower (Fig. 6 *D*). Holding the external

concentration constant at either 60 or 300 mM Cl produced a similar stimulation of Cl influx (outward currents) as the internal concentration was increased.

This action of internal Cl to increase Cl influx might have resulted from: (*a*) water flow induced by the imposed osmotic gradient, (*b*) an alteration of conductance due

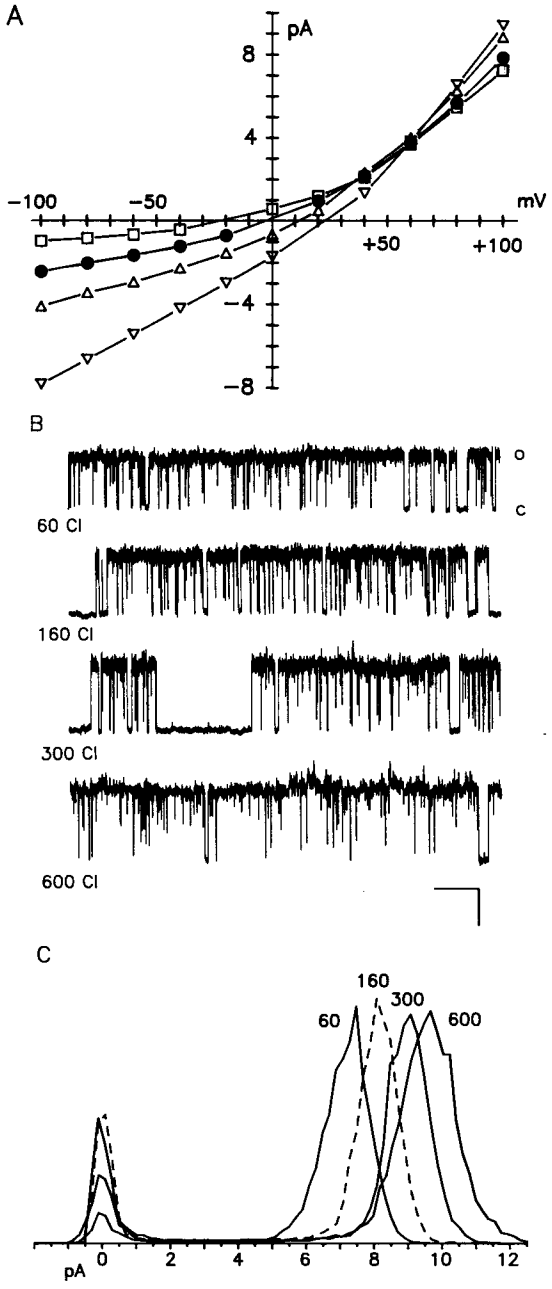

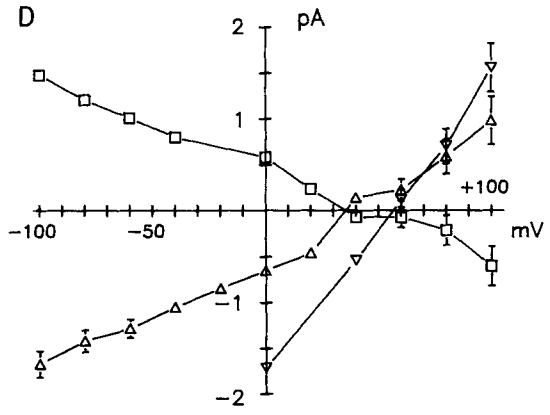

FIGURE 6. Single channel currents with Cl gradients: constant external Cl. (*A*) Current–voltage relations are shown at an external Cl concentration of 160 mM and internal Cl concentrations of 60 (□) n = 5, 160 (●) n = 26, 300 (△) n = 3, and 600 (▽) n = 3. (*B*) Single channel currents at +100 mV are shown with 160 mM NaCl pipette solution and bath solutions of 60, 160, 300, and 600 mM NaCl concentration. The scale bar represents 100 ms and 5 pA. (*C*) Amplitude histograms are shown for these currents. (*D*) Difference currents were calculated by subtracting the current–voltage relation with symmetric 160 Cl from the paired current–voltage relation obtained with a gradient.

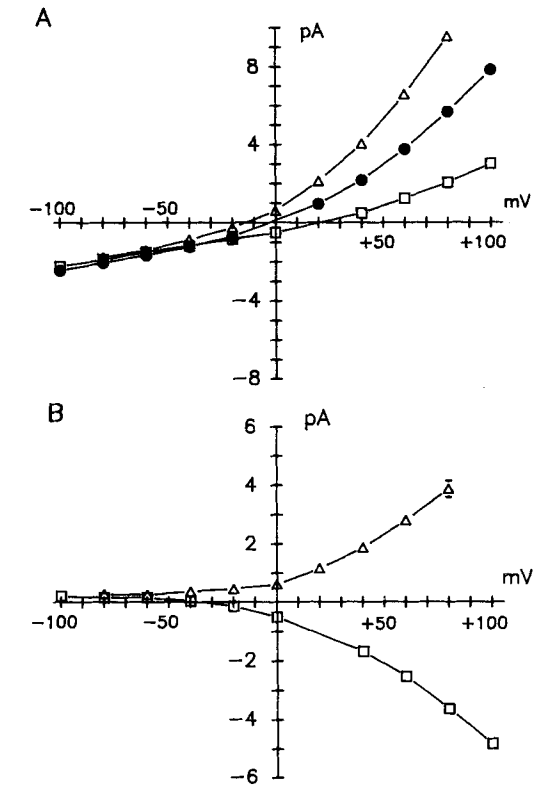

FIGURE 7. Single channel currents with Cl gradients: constant internal Cl. (*A*) Current–voltage relations are shown at an internal Cl concentration of 160 mM and external Cl concentrations of 60 (□) n = 8, 160 (●) n = 26, and 300 (△) n = 8. (*B*) Difference currents were calculated by subtracting the current–voltage relation with symmetric 160 Cl from the paired current–voltage relation obtained with a gradient.

to ionic strength screening of surface charges, or (*c*) an interaction of Cl with the channel at a site on the cytoplasmic face of the channel or in the conduction pathway. The osmotic gradient with internal 300 mM NaCl and external 160 mM NaCl would favor water influx, whereas the gradient with internal 60 mM NaCl and external 160 mM would favor water efflux. If water flow entrains ions in this Cl channel, as occurs in the gramicidin channel (Finkelstein and Rosenberg, 1979), then the osmotic

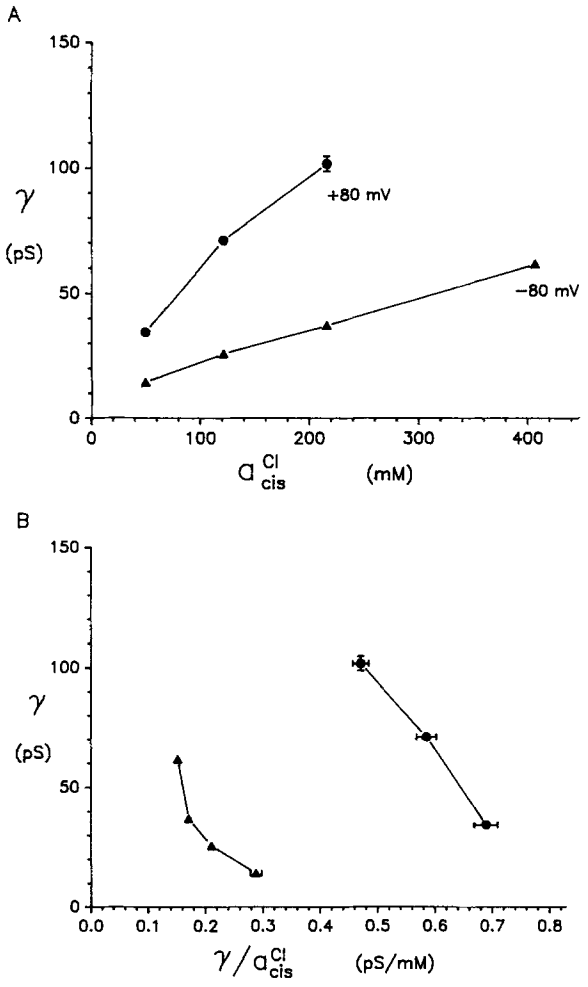

FIGURE 8. Dependence of single channel conductance on Cl activity: asymmetric Cl. (*A*) Conductance–activity relations are plotted from chord conductances calculated with currents at +80 mV (●), Fig. 7, and at −80 mV (▲), Fig. 6. (*B*) Eadie-Hofstee plots of the activity dependence are shown.

gradient might account for the *trans* stimulation. However, an osmotic gradient imposed by adding 250 mM sucrose to the bath favored water influx but did not alter single channel conductance, suggesting that water flow did not account for the alteration of Cl flow under conditions of osmotic gradients. The current–voltage relation with increased ionic strength (symmetric 160 NaCl + 150 Na gluconate) was identical to the current–voltage relation with symmetric 160 NaCl, indicating that

screening of surface charges was not responsible for *trans* stimulation. At this constant ionic strength, *trans* stimulation by internal Cl was abolished, which might result from competition between Cl and gluconate for a modifier site. Although the mechanism for *trans* stimulation of Cl influx is not completely clear, actions at the internal side of the channel can alter Cl influx as was seen also with changes of internal pH (Fig. 2).

Interaction between Permeant Anions

Differences between relative permeability and conductance estimates for many anions (Table I), together with deviations from independence (Figs. 5 *C* and 8) suggest that anions may reside in the channel long enough to interact with other permeating anions. Multiple occupancy within the amino acid gated Cl channels of neurons was suggested by anomolous mole fraction behavior of Cl and SCN (Bormann, Hamill, and Sakmann, 1987). A similar experiment is shown in Fig. 9 using Cl and SCN, which both have high permeability (Table I). Maintaining the total anion concentration constant, single channel conductance was measured at four mole fractions of Cl and SCN: 0.0, 0.2, 0.7, and 0.93. The single channel conductance was lowest when the mole fraction of SCN was 0.2 (Fig. 9 *A*). A distinct minimum in the mole fraction dependence (Fig. 9 *B*) is anomolous, assuming that the two anions do not interact in passing through the channel. Inhibitory interaction of this type, in which two highly permeant ions combine to produce less current than predicted, assuming independent flow, is consistent with a channel that allows multiple occupancy such that the presence of an ion in the channel alters occupation of the other sites and thereby channel conductance (Hille and Schwarz, 1978). The region of most pronounced inhibition was between −20 and +80 mV, but conductances at more negative potentials also did not conform to the expectations for a one-site model.

Other permeant anions also appear to alter channel conductance for Cl. These interactions were seen in the Cl influx (outward currents) from the experiments with anion substitution in the bath (internal side). Many of the less permeant anions appeared to block Cl influx, as shown by the single channel currents and amplitude histograms (Fig. 10, *A* and *B*). The differences in current between the condition with symmetric Cl (pipette and bath, 160 mM) and the condition with the substitute anions are shown in Fig. 10 *C*. Positive currents at negative potentials occur for ions that are less conductive than Cl (see Table I). The expectation for a simple channel obeying independence is that the difference current should approach zero at large positive potentials because external Cl carries the outward current. Hexanoate produced a large reduction in Cl influx (45 ± 5% decrease at +80 mV), which is illustrated by the negative difference current at positive potentials. In comparison, the similarly sized gluconate caused only a small and statistically insignificant reduction in Cl influx, which may reflect the reduction of internal Cl concentration rather than block. The other SCFAs did not inhibit Cl influx. Both pyruvate and lactate reduced Cl influx more than propanoate, suggesting that the presence of a polar group on these anions increased binding. Bicarbonate substitution also reduced Cl influx, and H_2PO_4 at a bath concentration of 100 mM (60 mM Cl) reduced influx at high positive potentials.

The more permeant anions had actions of two distinct types (Fig. 10 *D*). Both SCN and ClO_4 inhibited influx compared with stimulation by Br, I, and NO_3. These

divergent actions on Cl influx were observed even though these anions have similar relative permeabilities and conductances. Ionic strength was constant during these substitutions so that differences in surface charge screening were not involved in the *trans* inhibition or stimulation, supporting a direct action of anions at the internal side of the channel.

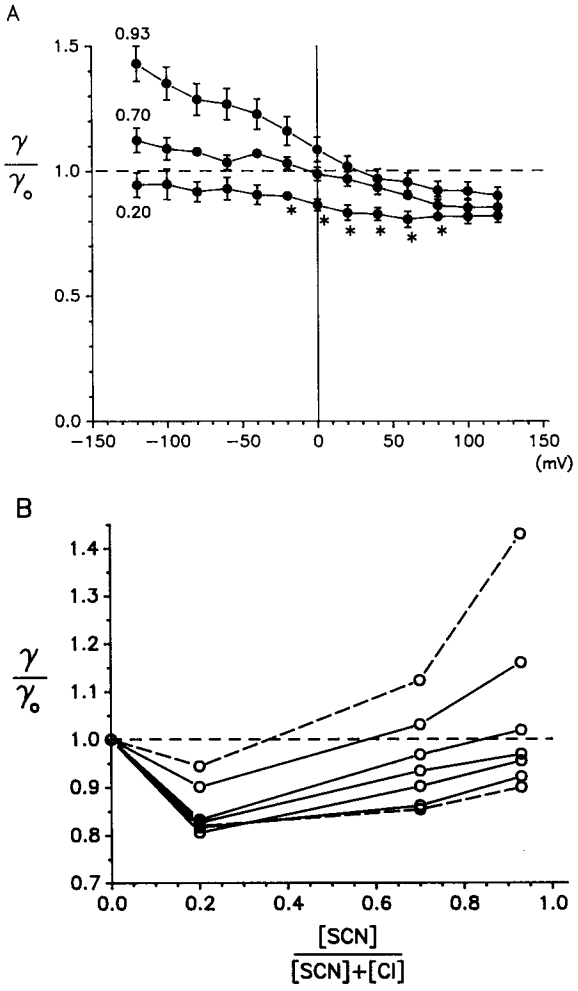

FIGURE 9. Dependence of single channel conductance on mole fraction of SCN. (*A*) Conductance–voltage relations are shown. Chord conductances relative to the case with 160 mM Cl (γ_o) were calculated for symmetric changes in the mole fraction of SCN: 0.2, 0.7, and 0.93 ($n = 4$). The total anion concentration ([Cl] + [SCN]) was 160 mM. Those relative conductances that are significantly lower ($P \leq 0.05$) than the relative conductances at mole fractions of both 0.0 and 0.93 are indicated (*). (*B*) The dependence of conductance on mole fraction is shown by plotting the relative conductances in *A* versus mole fraction. Curves from the extreme potentials are dashed (upper, −120 mV; lower, +120 mV). The potentials that exhibited a significant minimum are connected by solid lines (from top to bottom, −20, +20, +40, +60, and +80 mV).

The ability of anions to block Cl influx when present in the internal solution was in order of decreasing potency (at +100 mV): hexanoate (−0.32 ± 0.04), HCO_3 (−0.18 ± 0.03), TCA (−0.17 ± 0.03), TMA (−0.13 ± 0.03), H_2PO_4 (−0.12 ± 0.03), lactate (−0.11 ± 0.01), pyruvate (−0.10 ± 0.02), ClO_4 (−0.08 ± 0.03), 1-propaneSO_3 (−0.08 ± 0.01), and SCN (−0.07 ± 0.02). The plateau in the hexanoate difference current, and those for TCA and TMA, indicates relief of block as voltage was increased to more positive values. Only Br significantly stimulated Cl influx

(+0.05 ± 0.01), but NO_3 and I produced similar difference currents. Although these observations are consistent with anion interactions with the channel, the results do not allow a distinction to be made between interactions within the pore or at sites external to the conduction pathway.

DISCUSSION

Chloride secretion across epithelia proceeds via a Na-coupled cotransport entry mechanism in the basolateral membrane and a conductive exit mechanism in the apical membrane (Frizzell and Halm, 1990; Halm and Frizzell, 1990). Apical membrane Cl channels are a mandatory site of regulation for secretion, apparently opening only in the presence of secretory stimuli. The designation of the channel reported here as Cl conductive is supported by the anion selectivity shown in Table I and other observations (Giraldez, Murray, Sepúlveda, and Sheppard, 1989; Tabcharani, Jensen, Riordan, and Hanrahan, 1989) which indicate that physiologically relevant anions, HCO_3 and H_2PO_4 in particular, are relatively impermeant. The ability of HCO_3 to pass through this channel indicates that Cl and HCO_3 secretion may be stimulated concurrently, though Cl exit would predominate. In addition, the entry of other anions into the channel allows for kinetic modulation of Cl flow through the channel. Thus, this channel may serve primarily to allow Cl to exit across the apical membrane, but other anions may have a significant influence on the rate of Cl flow.

Voltage-dependent Single Channel Conductance

Outward rectification of the single channel current–voltage relation is one of the distinguishing features of this apical membrane Cl channel (Frizzell and Halm, 1990). Several properties of the channel could produce this rectification (Halm, Rechkemmer, Schoumacher, and Frizzell, 1988*b*). First, attenuation of single channel currents could result from filtering of rapid opening and closing kinetics, such that if the kinetics were voltage dependent then rectification would be apparent. Second, an asymmetric distribution of surface charges between the inner and outer leaflets of the plasma membrane or the internal and external sides of the channel protein could differentially change the concentration of permeant ions near the entrances to the channel, thereby altering the availability of ions for permeation. Third, structural features of the channel interior may cause a voltage dependence for passage through the pore.

Observed single-channel conductance can be reduced by the filtering characteristics of the recording system, as seen in the L-type Ca channel of excitable cells (Prod'hom, Pietrobon, and Hess, 1987; Pietrobon, Prod'hom, and Hess, 1989). Increasing pH to 9 or substituting H_2O with D_2O slowed the kinetics of this channel so that distinct conductance states could be observed. Decreasing temperature is another means of slowing channel gating kinetics. The activation energy for a conformational change, such as in gating, would be two to three times larger than that for ion diffusion (Hille, 1991). Cooling the channel, therefore, should produce a small drop in the rate of ion diffusion and a larger slowing of kinetics, such that the full current amplitude would become resolvable. An influence of gating (Fig. 1) would

be detected as a convergence of the conductance measured at negative voltages (lower curve) toward the conductance at positive voltages as the temperature was decreased; however, the relations for positive and negative voltages were parallel over a range of 30°C. Though an increase of current amplitude may occur below the

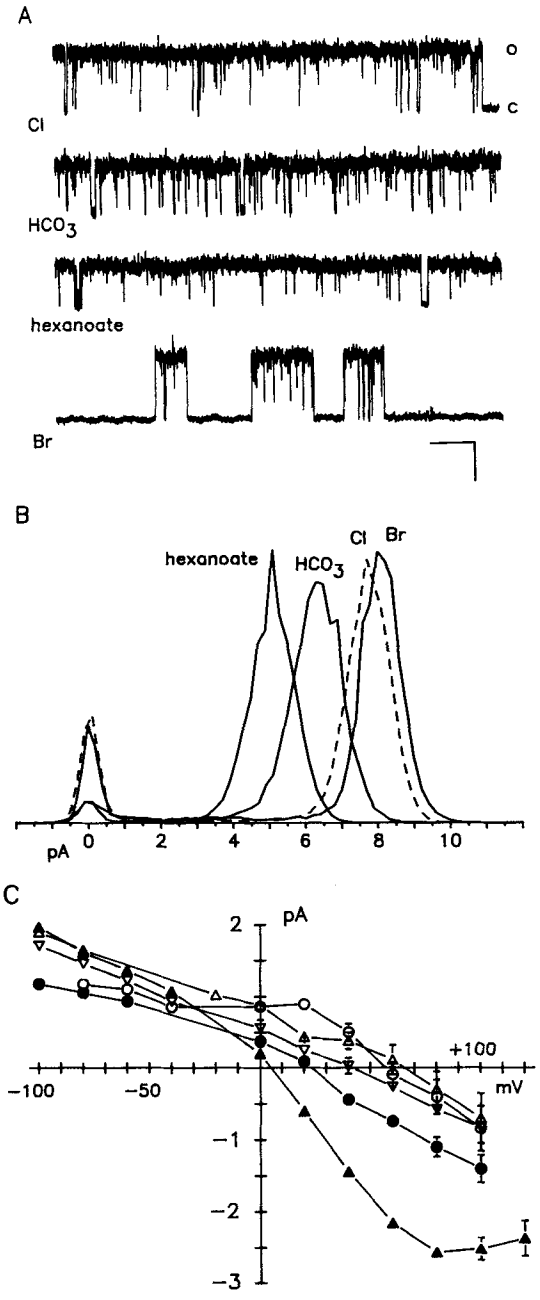

temperature range examined, these data suggest further that a gating process is not responsible for rectification of the current–voltage relation.

Rectification of current flow by preferential depletion of anions on one face of the channel (internal in this case) could be accomplished by surface charges, on the head groups of the bilayer lipids or directly on the channel protein (Dani and Eisenman, 1987). A similar Cl channel from colon (Reinhardt, Bridges, Rummel, and Lindemann, 1987) reconstituted into bilayers of neutral lipids exhibits outward rectification, suggesting that the source of fixed charges would have to be the channel or tightly associated native lipids. Screening the charges present on negative bilayer lipids with divalent cations (Moczydlowski, Alvarez, Vergara, and LaTorre, 1985) decreases the conductance of a reconstituted K channel, suggesting that the negative charges increase the local cation concentration. The increased ionic strength occur-

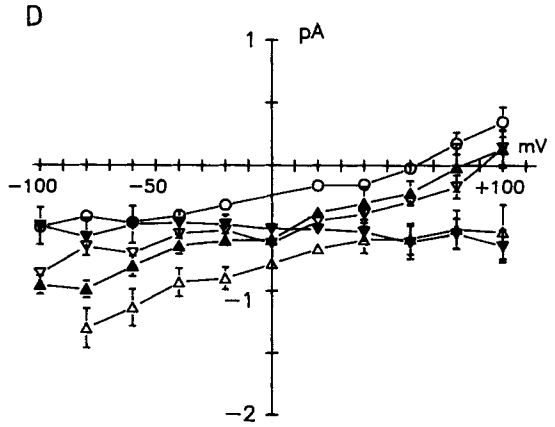

FIGURE 10. Anion interactions with Cl current. (*A*) Single channel currents at +100 mV are shown with 160 mM NaCl pipette solution and bath solutions with Cl substituted by other anions. The scale bar represents 100 ms and 5 pA. (*B*) Amplitude histograms are shown for these currents. (*C*) Difference currents are shown for internal substitution of Cl by anions with low permeability. The difference currents were calculated by subtracting the current–voltage relation with symmetric Cl from the paired current–voltage relation obtained with single-sided anion substitution. Positive currents at negative potentials indicate a lower relative conductance for the test anion, and negative currents at positive potentials indicate blocking of Cl influx by the test anion. The anions are: HCO_3 (●) $n = 5$, H_2PO_4 (○) $n = 3$, hexanoate (▲) $n = 3$, gluconate (△) $n = 4$, and lactate (▽) $n = 3$. (*D*) Difference currents are shown for internal substitution of Cl by anions with high permeability. The anions are: Br (○) $n = 14$, I (▽) $n = 11$, NO_3 (▲) $n = 9$, SCN (△) $n = 9$, and ClO_4 (▼) $n = 6$.

ring with the symmetrical increase in NaCl concentration (Fig. 5) would be expected to screen surface charges and diminish any ion rearrangement near the mouth of the channel. Similarity of rectification at different concentrations indicates that surface charge redistribution of ions was not a dominant factor in producing single channel rectification.

A complete explanation for rectification of current flow probably will require that an asymmetry exists in the free energy profile experienced by Cl as it flows through the pore of the channel. Imposition of an electric field across the channel illuminates asymmetries by accentuating different regions of the profile. A simple channel with one site and two barriers exhibits rectification if equally spaced barriers are of different heights or if equal-sized barriers are spaced unequally within the electric field (Krasne, 1978; Frizzell and Halm, 1990). In the case of asymmetric barrier

heights, the electric field will substantially reduce the effective height of the larger barrier only when this barrier is the last one crossed. In the case of asymmetric barrier position, the height of the barrier that is positioned only a small fraction of the distance into the electric field will be lowered substantially only when it is the last barrier crossed. Multi-site channels could exhibit rectification in a greater number of ways.

Anion Selectivity

The movement of ions through a channel involves replacement of ion–solvent interactions with ion–channel interactions (Wright and Diamond, 1977; Krasne, 1978; Eisenman and Horn, 1983; Hille, 1991). These interactions with the channel structure include steric influences since the ion must pass through the constriction of the pore. The relative permeabilities and conductances of the halide ions and other

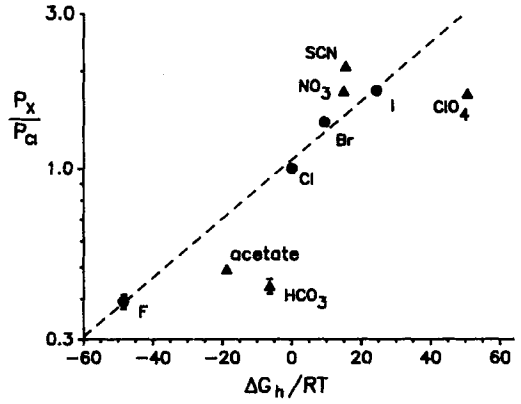

FIGURE 11. Relation of Cl channel permeability and hydration energy. Relative permeabilities are from Table I and free energies of hydration relative to that of Cl are from Wright and Diamond (1977). The relative free energies of hydration for SCN, HCO_3, H_2PO_4, and acetate were calculated from the relative enthalpy of hydration and an estimate of the relative entropy of hydration (Ball and Norbury, 1974; Wright and Diamond, 1977; Marcus, 1987). The relative free energy of hydration for H_2PO_4 is −52 RT. The relative permeabilities could be estimated from the halide relation (dashed line) for ClO_4 (3.06), SCN (1.47), NO_3 (1.45), HCO_3 (0.93), acetate (0.72), and H_2PO_4 (0.36), but these values deviate considerably from those measured.

inorganic anions (Figs. 3 and 4, Table I) do not conform to the equivalent conductances in aqueous solution, suggesting that the Cl channel is not a water-filled pore where interactions would be primarily between ions and water. The relation of relative permeabilities to hydration energies (Fig. 11) indicates that hydration forces are an important component of the barrier for ion entry into the channel. The spherically symmetric halides have a simple exponential relationship between relative permeability and hydration energy; however, several polyatomic anions deviate from this relation. Presumably the electrostatic configurations of NO_3 and SCN allow these ions to interact more favorably than a comparably sized halide anion. Interactions in the channel for HCO_3 and acetate must be less favorable. This halide selectivity sequence, dominated by hydration forces, implies that ion–channel interactions are relatively weaker than ion–water interactions, indicating a weak site in the terminology of Eisenman (Eisenman and Horn, 1983).

A possible structure for such an interaction site within the channel would be a fixed charge with a large radius or a relatively weak dipole (Wright and Diamond, 1977). Fixed positive charges in proteins can be found on the side chains of lysine, arginine, and histidine, and all of these charged groups are relatively large. In addition, many amino acids have polar side groups that might contribute to a weak interaction site: serine, threonine, tyrosine, asparagine, and glutamine. The peptide bond also is dipolar and could be oriented to form an anion interaction site. The departure of NO_3 and SCN from the halide dehydration relation (Fig. 11) may indicate that several groups coordinate with the anion at a selectivity site that favors anions capable of delocalizing charge in a specific shape. Nitrate differs in electrostatic configuration from HCO_3 (and the SCFAs) by having three identical oxygen atoms, rather than two, to share charge by resonance. A similar ability to delocalize negative charge by resonance exists for ClO_4 in comparison to the sulfonates and H_2PO_4 with, respectively, four, three, and two oxygens for resonance. These differences in electrical configuration and permeability (Fig. 3) suggest that optimal interaction at the selectivity site requires a coordination with multiple groups. Asymmetric anions such as HCO_3, H_2PO_4, and SCFAs would be less effective at coordinating with widely separated groups. Fluoride also would act as an asymmetric anion with incomplete dehydration interposing a water molecule between the anion and one of the charged groups. Coordination of cations within channels has been proposed to occur with an arrangement of multiple dipoles around the pore (Hille, 1991). Presumably in this Cl channel multiple dipoles would satisfy the constraints imposed by the expectation of a weak site better than multiple fixed charges.

Pore size. The minimum size of the pore for this Cl channel must put constraints on the largest anion that is permeable regardless of the relative ease in dehydration. The permeation of various anions suggests that the bore of the channel reaches a minimum diameter of 0.55–0.60 nm. In particular, TMA and TCA have geometric mean diameters of 0.60 and 0.62 nm, respectively, and were not detectably permeant. Although elongated anions should be constrained by this minimum aperture, longer side chains did not uniformly reduce relative permeability of SCFAs (Fig. 3), but relative conductance was lower for anions with longer side chains (Fig. 4). This difference suggests that these anions, butanoate and hexanoate in particular, pass through the channel by aligning the side chain with the axis of the pore and snaking along. The quasi-cylindrical diameter, therefore, appears to be the primary size constraint for entry, ~0.42 nm. A square aperture, similar to that proposed by Dwyer et al. (1980) for the acetylcholine receptor channel, of 0.50–0.55 nm on a side would also accept the permeant ions and exclude the large impermeant ions. Passage of 2-methyl-propanoate could occur along the diagonal, and to account for the minimal permeability of gluconate some hydrogen bonding with the channel structure would be necessary. The difference in relative permeability between ClO_4 and PF_6 (Fig. 3) suggests that the effective diameter of ClO_4 may also be reduced by formation of hydrogen bonds with the dipoles of the channel, similar to the case for hydroxylammonium and guanidinium in neuronal Na channels (Hille, 1971).

Anion conductance. Anion flow through this channel exhibits voltage-dependent conductance, probably as the result of an asymmetric free energy profile. The mole fraction behavior between Cl and SCN (Fig. 9) and concentration dependence at

negative potentials (Fig. 5) are consistent with multi-site free energy profiles. Conclusive evidence for the presence of more than one site (Begenisich and DeWeer, 1980) would consist of unidirectional flux ratios for Cl with a steep dependence on electrochemical gradient. A two-site, three-barrier model was fit to the single channel current data and yields elements expected for rectified flow (Fig. 12). Barriers and wells equally spaced in the electric field show an asymmetry in energies with the inner barrier higher than the outer barrier. Asymmetric placement of the barriers toward the interior still required similar differences in barrier heights to allow a fit. A deeper inner well is a feature that also was necessary to describe rectification of Cs flow through the calcium-activated K channel of sarcoplasmic reticulum (Cukierman, Yellen, and Miller, 1985). This model for Cl flow, in addition, can account qualitatively for the lower affinity of Cl during efflux compared with influx (Fig. 8), because negative potentials greatly enhance Cl exit from the channel to the external solution,

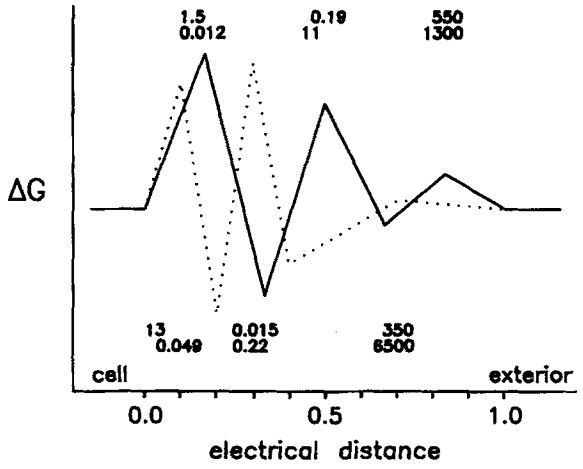

FIGURE 12. Free energy profiles for Cl flow. Eyring rate equations were used to fit the current flow through this Cl channel to hypothetical three-barrier, two-site models. The relative free energies illustrate the best fits to cases with evenly spaced barriers (solid line) and asymmetrically spaced barriers (dotted line). Forward (left to right) and reverse (right to left) rate constants are shown for each barrier in femtoequivalents per second. The upper set of rates is for even barrier spacing and the lower set is for asymmetric spacing, with the top and bottom values in each corresponding to forward and reverse, respectively.

thereby keeping the channel unoccupied. Blockers that occupy the sites would strengthen this model by indicating the positions of the wells within the electric field.

The ion selectivity of a channel results from differences in the free energy profiles for each ion. Differences in relative selectivity obtained from reversal potential shifts and single channel conductance (Fig. 4 *D*) occur because these two measures of permeation emphasize different features of the permeation pathway. Whereas permeability measurements are strongly influenced by barrier heights, the conductance of an ion depends on both barrier heights and well depths (Hille, 1991). The lower relative conductances compared with permeabilities suggest that several of the anions with high permeability (I, SCN, ClO_4, Br) reside in the channel for a comparatively long time. This pattern of permeation implies that the interaction sites at the barriers and wells are similar, with the wells providing slightly better coordination of the anions, so that the anions with higher permeabilities would have

lower barrier energies to overcome but also deeper wells to escape. Greater affinity of the permeant anions may account for the narrowing in the range of relative conductances at positive potentials (Fig. 4 *B*), with prolonged occupancy limiting flow (Fig. 12). Nitrate has both high permeability and high conductance, consistent with low barrier energies and comparatively high well energies, suggesting that the structure of the wells may differ in some feature from that at the barriers.

Although surface charges do not appear to account for rectification of single channel conductance, the presence of a positively charged group near the internal entrance to the channel is suggested by the pH dependence (Fig. 2). This charged group could be represented (Dani, 1986) by a minor well on the cell side of the energy diagram (Fig. 12). The increase in single channel conductance with reduced pH (Fig. 2) is consistent with a protonation that leads to higher Cl concentrations near the entrance of the channel. Histidine is a possible candidate for supplying the charged group, based on the pK_a (6.5) for the imidazolium side chain. The shallow dependence of Cl influx on internal pH suggests that this internal titration did not simply reduce the conductance of the pore, but rather has an asymmetric action on anion passage.

Anion–Anion Interactions

Flow of a Cl ion through this channel depends not only on interactions with the structural components but also with other anions. The mole fraction experiment with Cl and SCN (Fig. 9) indicates that the presence of two highly permeant anions can hinder net anion flow. This inhibitory action of SCN in the presence of Cl is not due to simple block of the channel because SCN has high conductance. If the multiple interaction sites are all within the pore, then the channel could be simultaneously occupied by two or more anions. The conduction pathway, in this case, would be similar to that described for the L-type calcium channel (Tsien, Hess, McCleskey, and Rosenberg, 1987), the delayed rectifier K channel (Yellen, 1987), and the TTX-sensitive sodium channel (Begenisich, 1987). The position of the minimum in the mole fraction relation (Fig. 9 *B*) at 0.2 indicates that SCN has a higher affinity than Cl, so that the possibility of mixed occupancy of the channel (Cl:SCN or SCN:Cl) is most likely at low mole fractions of SCN. The proposed energy profile for this Cl channel (Fig. 12) is consistent with the strong mole fraction effect at positive voltages (Fig. 9) where the barriers would have similar absolute heights contributing to the retention of anions within the channel. This result is similar to the concentration-dependent mole fraction effect in the L-type Ca channel (Campbell, Rasmussen, and Strauss, 1988; Friel and Tsien, 1989), in which interactions between different types of ions will be apparent only under conditions when the channel is at least singly occupied but not always doubly occupied. Although multiple occupancy may not be essential for imparting selectivity, as occurs in the L-type Ca channel, the possibility of interactions between different anions would allow for modulation of Cl flow.

Reductions in current (Fig. 10 *C*) seen with addition of less permeant anions (HCO_3, lactate, pyruvate, hexanoate) probably represents block simply by prolonged occupation of a site in the channel. Hexanoate may block in a folded conformation, which has similar dimensions to TCA and TMA, by acting as a plug at a narrow point in the pore. Attenuation at large positive potentials of the block by hexanoate, TCA,

and TMA may occur as knock-out by incoming Cl rather than by a potential-dependent exit of the blocker.

Although block of this channel by HEPES was not apparent in this study, the ability of anionic buffers to block anion channels (Yamamoto and Suzuki, 1987; Hanrahan and Tabcharani, 1990) is consistent with the observations of block by high concentrations of organic anions (Fig. 10 *C*). Because the sulfonates can enter this channel and many buffers have sulfonate-containing side chains, these molecules must be considered possible blockers of any anion channel.

All of the interactions between anions were not inhibitory. Stimulation of Cl influx at constant ionic strength by internal Br (Fig. 10 *D*) is consistent with the *trans* stimulation of Cl influx by internal Cl (Fig. 6 *D*) occurring as a direct action of Cl. The lack of *trans* stimulation with extracellular Cl suggests that this stimulatory action occurs with occupation of a site near the cytoplasmic end of the channel. The higher conductances for influx produced by symmetric Cl concentration increase (Fig. 5 *B*) compared with single-sided increase (Fig. 8 *A*) may have occurred because internal Cl stimulated Cl influx above the level determined simply by the external Cl concentration. Whether the stimulatory modifier site for conductance exists on the internal side of the channel or within the pore cannot be determined with the present data.

Chloride Channels

This Cl channel, observed in secretory epithelia (Gögelein, 1988; Frizzell and Halm, 1990), has several similarities with other types of channels. The estimated size of the pore is similar to that estimated for the GABA receptor Cl channel (Bormann et al., 1987), the acetylcholine receptor channel (Dwyer et al., 1980), and the L-type calcium channel (Tsien et al., 1987). In part, the rather large size of the acetylcholine receptor channel is a reason for its lack of preference between cations. Any Cl channel, however, would have to be rather large because of the ionic diameter of Cl (larger than that of Cs, 0.34 nm). Exclusion of small organic anions, therefore, is difficult because steric restrictions alone may not provide discrimination. For this epithelial Cl channel and the GABA receptor Cl channel, which has the same general selectivity pattern (Bormann et al., 1987), distinctions between anions of similar size are apparently made by favoring the anions capable of delocalizing charge.

A channel structure that excludes asymmetric anions such as HCO_3 and H_2PO_4 also would reduce hydroxyl ion flow, which may be a reason for the common occurrence of this selectivity pattern (Frizzell and Halm, 1990). Only the protein P Cl channel from *Pseudomonas aeruginosa* (Benz and Hancock, 1987) may have a high field strength site, as indicated by high relative permeation of F. The Cl channels from electroplax (Miller and White, 1980; Kanemasa, Banba, and Kasai, 1987) and the basolateral membrane of thick ascending limb cells (Paulais and Teulon, 1990) both prefer Cl over Br; but the low permeability for F in these channels suggests that the selectivity region also may be a weak site, together with steric restrictions excluding anions larger than Br. Because Cl is the only symmetrical anion of those physiologically relevant (HCO_3, H_2PO_4, OH, and organic anions), exclusion of asymmetric anions becomes a simple means to provide selective anion permeation.

Measurements of secretion across the tracheal epithelium during substitution of bath solution Cl with Br or I indicate that Cl is preferentially transported (Widdi-

combe and Welsh, 1980). The epithelial selectivity sequence of Cl (1.0) > Br (0.7) ≫ I (0.0) matches that for the Na:K:2Cl cotransporter in the basolateral membrane (Halm and Frizzell, 1990), but is far from the conductance sequence seen for anion efflux through this channel (Table I) or tracer efflux from stimulated epithelial monolayers (Venglarik, Bridges, and Frizzell, 1990). Anion selection during secretion will involve both the anion uptake and exit steps; and the restrictive selectivity at the basolateral membrane uptake process apparently dominates the selection of anions to be secreted.

Currently, single channel conductance is used to distinguish among the chloride channels activated by secretagogues in epithelia. Interestingly, making the outer barrier similar in height to the inner barrier (Fig. 12) results in a nearly ohmic single channel conductance of 10–20 pS, which is similar to the channels reported by Tabcharani et al. (1990) and Duszyk et al. (1990). Whether the height of this outer barrier could be regulated to alter Cl flow remains to be determined.

Interactions between anions may exert influence on secretory Cl flow as the metabolic state causes alterations in lactate and HCO_3 concentration. Metabolic acidosis occurs with increased lactate production, such that an increase of channel conductance with acidic pH may balance the blocking action of lactate. Perhaps more relevant to anion secretion is the state of HCO_3 interactions with this Cl channel. The extent to which increased HCO_3 activity at basic pH could reduce Cl flow depends on the ability of the cell to regulate cell pH, but this regulation also would determine the rate of HCO_3 secretion that occurs through this channel. Whether these interactions have physiological relevance must be tested, but these effects do illustrate some of the interactions that occur as anions flow through the channel and the structural features in the process of anion permeation.

We thank J. Brugge for cell culture, E. Walthall for data analysis, Dr. O. Alvarez for a computer program to calculate free energy profiles, and Dr. R. Bridges and Dr. T. Begenisich for helpful suggestions in preparing the manuscript.

This work was supported by National Institutes of Health grants DK-31091 and DK-39007.

Original version received 10 October 1990 and accepted version received 26 November 1991.

REFERENCES

Ball, M. C., and A. H. Norbury. 1974. Physical Data for Inorganic Chemists. Longman, London. 52–57.

Bamberg, E., and P. Läuger. 1974. Temperature dependent properties of gramicidin A channel. *Biochimica et Biophysica Acta.* 367:127–133.

Begenisich, T. 1987. Molecular properties of ion permeation through sodium channels. *Annual Review of Biophysics and Biophysical Chemistry.* 16:247–263.

Begenisich, T., and P. DeWeer. 1980. Potassium flux ratio in voltage-clamped squid giant axons. *Journal of General Physiology.* 76:83–98.

Benz, R., and R. E. W. Hancock. 1987. Mechanism of ion transport through the anion-selective channel of *Pseudomonas aeruginosa* outer membrane. *Journal of General Physiology.* 89:275–295.

Bormann, J., O. P. Hamill, and B. Sakmann. 1987. Mechanism of anion permeation through channels gated by glycine and γ-aminobutyric acid in mouse cultured spinal neurones. *Journal of Physiology.* 385:243–286.

Campbell, D. L., R. L. Rasmussen, and H. C. Strauss. 1988. Theoretical study of the voltage and concentration dependence of the anomolous mole fraction effect in single calcium channels. New insight into the characteristics of multi-ion channels. *Biophysical Journal.* 54:945–954.

Cliff, W. H., and R. A. Frizzell. 1990. Separate chloride conductances activated by cyclic-AMP and calcium in chloride secreting epithelial cells. *Proceedings of the National Academy of Sciences, USA.* 87:4956–4960.

Cukierman, S., G. Yellen, and C. Miller. 1985. The potassium channel of sarcoplasmic reticulum. A new look at cesium block. *Biophysical Journal.* 48:477–484.

Dani, J. A. 1986. Ion channel entrances influence permeation. Net charge, size, shape and binding considerations. *Biophysical Journal.* 49:607–618.

Dani, J. A., and G. Eisenman. 1987. Monovalent and divalent cation permeation in acetylcholine receptor channels. Ion transport related to structure. *Journal of General Physiology.* 89:959–983.

Duszyk, M., A. S. French, and S. F. P. Man. 1990. The 20-pS chloride channel of the human airway epithelium. *Biophysical Journal.* 57:223–230.

Dwyer, T. M., D. J. Adams, and B. Hille. 1980. The permeability of the end plate channel to organic cations in frog muscle. *Journal of General Physiology.* 75:469–492.

Eisenman, G., and R. Horn. 1983. Ionic selectivity revisited: the role of kinetic and equilibrium processes in ion permeation through channels. *Journal of Membrane Biology.* 76:197–225.

Finkelstein, A., and P. A. Rosenberg. 1979. Single-file transport: implications for ion and water movement through gramicidin A channels. *Membrane Transport Processes.* 3:73–88.

Friel, D. D., and R. W. Tsien. 1989. Voltage-gated calcium channels: direct observation of the anomalous mole fraction effect at the single-channel level. *Proceedings of the National Academy of Sciences, USA.* 86:5207–5211.

Frizzell, R. A., and D. R. Halm. 1990. Chloride channels in epithelial cells. *Current Topics in Membranes and Transport.* 37:247–282.

Giraldez, F., K. J. Murray, F. V. Sepúlveda, and D. N. Sheppard. 1989. Characterization of a phosphorylation-activated Cl-selective channel in isolated *Necturus* enterocytes. *Journal of Physiology.* 416:517–537.

Gögelein, H. 1988. Chloride channels in epithelia. *Biochimica et Biophysica Acta.* 947:521–547.

Green, W. N., L. B. Weiss, and O. S. Andersen. 1987. Batrachotoxin-modified sodium channels in planar lipid bilayers. Ion permeation and block. *Journal of General Physiology.* 89:841–872.

Halm, D. R., and R. A. Frizzell. 1990. Intestinal chloride secretion. *In* Textbook of Secretory Diarrhea. E. Lebenthal and M. Duffey, editors. Raven Press, Ltd., New York. 47–58.

Halm, D. R., G. R. Rechkemmer, R. A. Schoumacher, and R. A. Frizzell. 1988*a*. Apical membrane chloride channels in a colonic cell line activated by secretory agonists. *American Journal of Physiology.* 254. (*Cell Physiology* 23):C505–C511.

Halm, D. R., G. R. Rechkemmer, R. A. Schoumacher, and R. A. Frizzell. 1988*b*. Biophysical properties of a chloride channel in the apical membrane of a secretory epithelial cell. *Comparative Biochemistry and Physiology.* 90A:597–601.

Hanrahan, J. W., and J. A. Tabcharani. 1990. Inhibition of an outwardly rectifying anion channel by HEPES and related buffers. *Journal of Membrane Biology.* 116:65–77.

Hille, B. 1971. The permeability of the sodium channel to organic cations in myelinated nerve. *Journal of General Physiology.* 58:599–619.

Hille, B. 1991. Ionic Channels of Excitable Membranes. Sinauer Associates, Inc., Sunderland, MA. 607 pp.

Hille, B., and W. Schwarz. 1978. Potassium channels as multi-ion single-file pores. *Journal of General Physiology.* 72:409–442.

Kanemasa, T., K. Banba, and M. Kasai. 1987. Voltage-gated anion channel of the electric organ of *Narke japonica* incorporated into planar bilayers. *Journal of Biochemistry.* 101:1025–1032.

Krasne, S. 1978. Ion selectivity in membrane permeation. Physiology of Membrane Disorders. T. E. Andreoli, J. F. Hoffman, and D. D. Fanestil, editors. Plenum Publishing Corp., New York. 217–241.

Läuger, P. 1973. Ion transport through pores: a rate-theory analysis. *Biochimica et Biophysica Acta.* 311:423–441.

Li, M., J. D. McCann, C. M. Liedtke, A. C. Nairn, P. Greengard, and M. J. Welsh. 1988. Cyclic-AMP-dependent protein kinase opens chloride channels in normal but not cystic fibrosis airway epithelium. *Nature.* 331:358–360.

Marcus, Y. 1987. The thermodynamics of solvation of ions. *Journal of the Chemical Society, Faraday Transactions.* 83:339–349.

Miller, C., and M. M. White. 1980. A voltage-dependent chloride conductance channel from *Torpedo* electroplax membrane. *Annals of the New York Academy of Sciences.* 341:534–551.

Moczydlowski, E., O. Alvarez, C. Vergara, and R. LaTorre. 1985. Effect of phospholipid surface charges on the conductance of a calcium activated potassium channel in planar lipid bilayers. *Journal of Membrane Biology.* 83:273–282.

Paulais, M., and J. Teulon. 1990. Cyclic-AMP-activated chloride channel in basolateral membrane of the thick ascending limb of the mouse kidney. *Journal of Membrane Biology.* 113:253–260.

Pietrobon, D., B. Prod'hom, and P. Hess. 1989. Interactions of protons with single open L-type calcium channels. pH dependence of proton-induced current fluctuations with cesium, potassium and sodium as permeant ions. *Journal of General Physiology.* 94:1–21.

Prod'hom, B., D. Pietrobon, and P. Hess. 1987. Direct measurement of proton transfer rates to a group controlling the dihydropyridine-sensitive calcium channel. *Nature.* 329:243–246.

Reinhardt, R., R. J. Bridges, W. Rummel, and B. Lindemann. 1987. Properties of an anion-selective channel from rat colonic enterocytes plasma membranes reconstituted into planar phospholipid bilayers. *Journal of Membrane Biology.* 95:47–54.

Robinson, R. A., and R. H. Stokes. 1970. Electrolyte Solutions. Butterworth & Co., Ltd., London. 118–132.

Schoumacher, R. A., R. L. Shoemaker, D. R. Halm, E. A. Tallant, R. W. Wallace, and R. A. Frizzell. 1987. Phosphorylation fails to activate chloride channels from cystic fibrosis airway cells. *Nature.* 330:752–754.

Stewart, C. P., J. M. Winterhager, K. Heintze, and K. Peterson. 1989. Electrogenic bicarbonate secretion by guinea pig gallbladder epithelium: apical membrane exit. *American Journal of Physiology.* 256 (*Cell Physiology* 25):C736–C749.

Tabcharani, J. A., T. J. Jensen, J. R. Riordan, and J. W. Hanrahan. 1989. Bicarbonate permeability of the outwardly rectifying anion channel. *Journal of Membrane Biology.* 112:109–122.

Tabcharani, J. A., W. Low, D. Elie, and J. W. Hanrahan. 1990. Low conductance chloride channel activated by cyclic-AMP in the epithelial cell line T84. *FEBS Letters.* 270:157–164.

Tsien, R. W., P. Hess, E. W. McCleskey, and R. L. Rosenberg. 1987. Calcium channels: mechanisms of selectivity, permeation and block. *Annual Review of Biophysics and Biophysical Chemistry.* 16:265–290.

Venglarik, C. J., R. J. Bridges, and R. A. Frizzell. 1990. A simple assay for agonist-regulated chloride and potassium conductances in salt-secreting epithelial cells. *American Journal of Physiology.* 259 (*Cell Physiology* 28):C358–C364.

Widdicombe, J. H., and M. J. Welsh. 1980. Anion selectivity of the chloride-transport process in dog tracheal epithelium. *American Journal of Physiology.* 239 (*Cell Physiology* 8):C112–C117.

Wright, E. M., and J. M. Diamond. 1977. Anion selectivity in biological systems. *Physiological Reviews.* 57:109–156.

Wrong, O. M., J. Edmonds, and V. S. Chadwick. 1981. The Large Intestine: Its Role in Mammalian Nutrition and Homeostasis. MTP Press Ltd., Lancaster, UK. 25.

Yamamoto, D., and N. Suzuki. 1987. Blockage of chloride channels by HEPES buffer. *Proceedings of the Royal Society of London B.* 230:93–100.

Yellen, G. 1987. Permeation in potassium channels: implications for channel structure. *Annual Review of Biophysics and Biophysical Chemistry.* 16:227–246.